

# Alternative approaches to the numerical calculation of impedance

N. Ida

In many practical applications of numerical analysis applied to low-frequency electromagnetic problems, the desired output is often in terms of coil impedance. The mesh variable calculated by the more commonly used numerical formulations is the magnetic vector potential from which quantities like field intensities, eddy currents and others are calculated. In nondestructive testing applications, the quantity of interest is often the impedance of a coil or an array of coils. This paper discusses the calculation of impedance as a post-processing computation and introduces a new method of calculation of impedances and inductances based on computation of energy in the finite element mesh. The results presented clearly show the advantage of using direct integration methods for 2D and axisymmetric geometries. The energy approach, while valid regardless of dimensionality, should be restricted to 3D applications. Multiple-coil configurations in 3D applications present a special problem in analysis. The total impedance or inductance can be easily calculated but not independent coil or differential impedances. A method for calculation of these quantities in 3D computations is also presented.

**Keywords:** numerical analysis, coil impedance, coil inductance, axisymmetric and three-dimensional applications

The use of auxiliary functions, vectors or scalars, to simplify Maxwell's equations is a widespread practice in the numerical solution of electromagnetic field problems<sup>[1]</sup>. This also means that in most cases the quantity of interest is not found directly and one has to perform additional calculations to reach the final result.

In particular, the magnetic vector potential is very popular both in two<sup>[2-4]</sup> and three-dimensional<sup>[5-7]</sup> calculations, yet it is of little practical use by itself. Although any magnetic quantity is calculable from the magnetic vector potential, one must be concerned with such considerations as errors introduced due to additional calculations and the relative merits of alternative formulations. It is also possible that a particular approach will work well in some situations and fail in others, or it may be suitable for 2D calculations but not for 3D applications.

A point in case is the calculation of NDT eddy current probe impedances. The impedance can be calculated by direct integration over the coils' cross-sectional areas directly from the distribution of the magnetic vector potential. Alternatively, the stored and dissipated energy in the system can be calculated first, and then the impedance. Moreover, the first approach is only feasible in 2D or axisymmetric applications. The energy approach is more general and applicable to 3D problems as well.

Integrating the magnetic vector potential over a coil's cross section allows the calculation of impedances for

each part of a multiple-coil arrangement. Calculation of energies can only be done for the whole system and only the total impedance is calculable.

The impedance in 2D or axisymmetric problems solved by finite elements is normally calculated on the basis of direct (line) integration around the source<sup>[4, 8]</sup>. It assumes, implicitly, that the magnetic vector potential is constant in the circumferential direction (*ie* for a coil) or along the source (*ie* for a 2D source distribution). This method cannot be extended to 3D applications. A new method is therefore proposed based on calculation of the stored and dissipated energies in the solution domain. From these energies, the real and imaginary parts of the impedance are then calculated.

This paper deals specifically with the calculation of coil inductances and impedances as they relate to eddy current NDT in axisymmetric and three-dimensional applications. The two basic methods for calculation of inductance (and therefore impedance) are evaluated first for a simple coil in axisymmetric and three dimensions and then for a differential eddy current probe. It is shown that for axisymmetric applications either method is satisfactory.

In 3D applications, however, the energy approach is a necessity but has some restrictions in terms of range of applications. The calculation of differential impedances of eddy current probes or the calculation of inductances or impedances of part of a multiple system of coils presents a

unique problem: one cannot associate part of the energy with a particular coil or part of the sources. The only quantity that can be obtained is the total (stored and dissipated) energy. A method of solving this difficulty under some circumstances and for the calculation of differential probe impedances is also presented.

The results presented are compared with those of analytical calculations wherever possible.

### Field equations and calculation of the magnetic vector potential

The field equations describing low-frequency electromagnetic phenomena are derived from Maxwell's equations. The derivation is not repeated here, but it is useful to look at the general, steady-state (linear or non-linear) equations written using phasor notation for the magnetic vector potential  $A^{[7]}$ :

$$\nabla \times (\nu \nabla \times \mathbf{A}) = \mathbf{J}_s - j\omega\sigma\mathbf{A} \quad (1)$$

where  $\omega$  is the angular frequency,  $\sigma$  the material conductivity and  $\nu = 1/\mu$  is the reluctivity of the material. For isotropic materials and assuming linearity, the general eddy current equation in phasor notation can be simplified to

$$\nu \nabla \times \nabla \times \mathbf{A} = \mathbf{J}_s - j\omega\sigma\mathbf{A} \quad (2)$$

Similarly, by removing the last term (the eddy current term), one obtains the 3D magnetostatic equation<sup>[6]</sup>

$$\nu \nabla \times \nabla \times \mathbf{A} = \mathbf{J}_s \quad (3)$$

Here  $\mathbf{A}$  and  $\mathbf{J}_s$  are real vectors as compared to the complex vectors in Equation (2).

In two-dimensional applications only one component of the current density  $\mathbf{J}_s$  and the magnetic vector potential  $\mathbf{A}$  exist. This further simplifies the equation<sup>[3,8]</sup>:

$$\nu \left( \frac{\partial^2 \mathbf{A}}{\partial x^2} + \frac{\partial^2 \mathbf{A}}{\partial y^2} \right) = -\mathbf{J}_s + j\omega\sigma\mathbf{A} \quad (4)$$

The  $z$  component is taken for convenience. Using similar arguments as for Equation (3), the 2D magnetostatic equation is

$$\nu \left( \frac{\partial^2 \mathbf{A}}{\partial x^2} + \frac{\partial^2 \mathbf{A}}{\partial y^2} \right) = -\mathbf{J}_s \quad (5)$$

Finally, in axisymmetric geometries, the eddy current and magnetostatic equations are<sup>[8]</sup>

$$\nu \left( \frac{\partial^2 \mathbf{A}}{\partial r^2} + \frac{1}{r} \frac{\partial \mathbf{A}}{\partial r} + \frac{\partial^2 \mathbf{A}}{\partial z^2} - \frac{\mathbf{A}}{r^2} \right) = -\mathbf{J}_s + j\omega\sigma\mathbf{A} \quad (6)$$

$$\nu \left( \frac{\partial^2 \mathbf{A}}{\partial r^2} + \frac{1}{r} \frac{\partial \mathbf{A}}{\partial r} + \frac{\partial^2 \mathbf{A}}{\partial z^2} - \frac{\mathbf{A}}{r^2} \right) = -\mathbf{J}_s \quad (7)$$

Regardless of which of the above equations one solves, a distribution of the magnetic vector potential is obtained throughout the region. This distribution is defined by nodal values of  $\mathbf{A}$  in a mesh. These values can be either complex (Equations (2), (4) and (6)) or real (Equations (3), (5) and (7)) and can have either a single component of  $\mathbf{A}$  at each node (Equations (4)–(7)) or three components (Equations (2) and (3)).

For the purpose of this work it will be assumed that the magnetic vector potential has been calculated using a finite element mesh. The axisymmetric results presented are based on the solution of Equation (6) or (7) in a triangular or quadrilateral mesh. The three-dimensional results are based on the solution of Equation (2) or (3) in an eight-node hexahedral element mesh.

The equations above and the finite element formulation in terms of the magnetic vector potential are assumed to result in a unique solution for the magnetic vector potential. Since this has a bearing on the calculations presented in this work, a brief discussion of the uniqueness aspect of the finite element formulations used is included in the appendix.

### Direct calculation of inductance and impedance

The impedance of a circular filament of radius  $r_i$  can be calculated directly from the distribution of the magnetic vector potential<sup>[8]</sup>:

$$Z_i = j\omega 2\pi r_i A_i / I_s \quad (8)$$

where  $I_s$  is the impressed current in the filament. Integration of Equation (8) over the turns in the cross section of a coil (or coils) yields the correct impedance. The impedance, the current density and the magnetic vector potential are complex quantities. The vector notation for the magnetic vector potential has been removed since in 2D geometries it is a single-component vector. With discrete values of  $\mathbf{A}$ , this simple scheme is not possible and a somewhat different approach is required. Considering first Figure 1a, the magnetic vector potential within the cross section of the coil is known only at nine discrete points. The simplest way to treat this problem is to assume for each element an average  $A_c$  and  $r_c$ . These values, known as the centroidal values, are calculated either as a simple average within each element

$$A_c = (A_I + A_J + A_K) / 3 \quad (9)$$

$$r_c = (r_I + r_J + r_K) / 3 \quad (10)$$

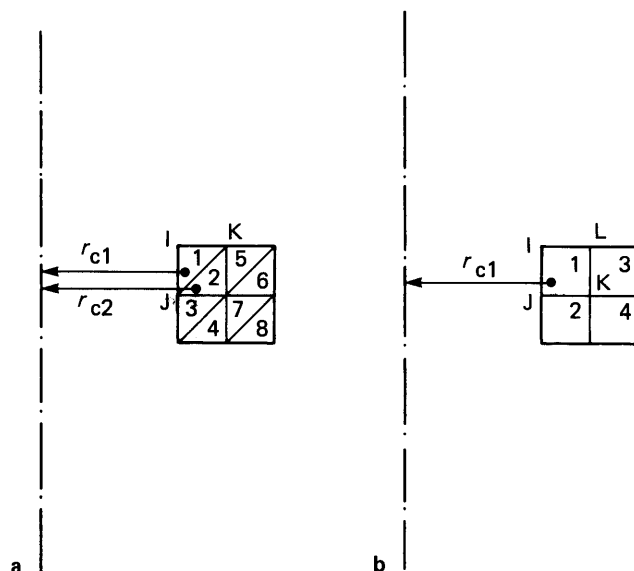


Fig. 1 Discretization of the coil and calculation of centroidal values: (a) triangular elements; (b) quadrilateral elements

or, with better accuracy<sup>[8]</sup>, as

$$A_c = \left[ \frac{1}{12} \left( A_I^2 + A_J^2 + A_K^2 + (A_I + A_J + A_K)^2 \right) \right]^{0.5} \quad (11)$$

$$r_c = \left[ \frac{1}{12} \left( r_I^2 + r_J^2 + r_K^2 + (r_I + r_J + r_K)^2 \right) \right]^{0.5} \quad (12)$$

where I, J and K are the three nodes of an element.

If the finite element chosen is that of Figure 1b, these simply become an average over four nodes:

$$A_c = (A_I + A_J + A_K + A_L)/4 \quad (13)$$

$$r_c = (r_I + r_J + r_K + r_L)/4 \quad (14)$$

Either way, if there are  $N_s$  turns in the area defined by element  $i$  and the area of this element is  $\Delta_i$ , one can write for the impedance of a coil contained in element  $i$  as

$$Z_i = j\omega 2\pi r_{ci} A_{ci} (N_s \Delta_i) / I_s \quad (15)$$

Summing this over all the elements in the coil's cross section, the impedance of the coil is obtained as

$$Z_{\text{coil}} = \frac{j\omega 2\pi N_s}{I_s} \sum_1^n r_{ci} A_{ci} \Delta_i \quad (16)$$

Since, in general, the turn density  $N_s$  is not readily calculable, one can write the impedance in terms of the current density in the coils,  $J_s (= N_s I_s)$ :

$$Z_{\text{coil}} = \frac{j\omega 2\pi J_s}{I_s^2} \sum_1^n r_{ci} A_{ci} \Delta_i \quad (17)$$

Similarly, for two coils connected differentially and carrying opposite, equal currents, one obtains

$$Z_{\text{probe}} = \frac{j\omega 2\pi J_s}{I_s^2} \left( \sum_1^{n_a} r_{ci} A_{ci} \Delta_i + \sum_1^{n_b} r_{ci} A_{ci} \Delta_i \right) \quad (18)$$

where  $n_a$  and  $n_b$  are the number of elements in the two coils. The self-inductance of a single coil can be calculated directly from Equation (17) as

$$L_{\text{coil}} = \frac{2\pi J_s}{I_s^2} \sum_1^n r_{ci} \Delta_i \text{Re}(A_{ci}) \quad (19)$$

and the inductance of a differential probe as

$$L_{\text{probe}} = \frac{2\pi J_s}{I_s^2} \left( \sum_1^{n_a} r_{ci} \Delta_i \text{Re}(A_{ci}) + \sum_1^{n_b} r_{ci} \Delta_i \text{Re}(A_{ci}) \right) \quad (20)$$

It is obvious that in magnetostatic situations the impedance in Equations (17) and (18) reduces to the DC resistance of the coil. This is, by definition of the finite element model<sup>[2,5]</sup>, zero. The inductance, however, is independent of frequency and Equations (19) and (20) still hold.  $\text{Re}(A_{ci})$  is now replaced by  $A_{ci}$ . It is interesting to note that an equivalent in 2D to the coil geometry is a long conductor or a system of conductors. Equation (17), for example, becomes

$$Z_{\text{cond}} = \frac{j\omega J_s}{I_s^2} \sum_1^n A_{ci} \Delta_i \quad (21)$$

while Equation (19) becomes

$$L_{\text{cond}} = \frac{J_s}{I_s^2} \sum_1^n A_{ci} \Delta_i \quad (22)$$

In these calculations the impedance or inductance is calculated directly from the magnetic vector potential and therefore no additional errors are introduced. Some errors are inevitable in the calculation of  $A_c$  and  $r_c$  as well as in the calculation of  $\Delta_i$ , but these can be made smaller by using a larger number of elements in the coil's cross section.

This approach is not suitable for 3D applications. In the calculation of impedance using Equation (8), the magnetic vector potential has been implicitly assumed to be constant along the circumference of the filament, as well as having a single component in the direction of the current. Neither of these assumptions is correct in 3D geometries and therefore the impedance must be calculated from relations that are independent of local variations in magnitude and direction of the magnetic vector potential.

## Calculation of inductances and impedances from energy considerations

The impedance of a source can be calculated from the energy of the system by associating its inductance with the stored energy and its resistance with the dissipated energy. Thus in Equation (1) the left-hand side represents the stored energy in the magnetic field, while the second term on the right-hand side is the eddy current density and therefore represents the dissipated energy.

The stored energy can be expressed as a volume integral:

$$W = \frac{1}{2} \int_{\nu} \mathbf{B} \cdot \mathbf{H} \, d\nu \quad (23)$$

Rewriting this in terms of the components of  $\mathbf{B}$  alone and assuming constant reluctivity in each spatial direction, the energy stored in a finite element of volume  $\nu_i$  can be written as<sup>[6]</sup>

$$W_i = \frac{1}{2} (\nu_x B_x^2 + \nu_y B_y^2 + \nu_z B_z^2) \nu_i \quad (24)$$

The flux density  $B$  is not known and has to be calculated from  $A$ :

$$\begin{aligned} B_x &= \frac{\partial A_z}{\partial y} - \frac{\partial A_y}{\partial z} \\ B_y &= \frac{\partial A_x}{\partial z} - \frac{\partial A_z}{\partial x} \\ B_z &= \frac{\partial A_y}{\partial x} - \frac{\partial A_x}{\partial y} \end{aligned} \quad (25)$$

Substituting this in Equation (24) and summing over all the elements in the solution region yields the total stored energy in the system:

$$\begin{aligned} W &= \frac{1}{2} \sum_1^N \left[ \nu_x \left( \frac{\partial A_{zi}}{\partial y_i} - \frac{\partial A_{yi}}{\partial z_i} \right)^2 \right. \\ &\quad \left. + \nu_y \left( \frac{\partial A_{xi}}{\partial z_i} - \frac{\partial A_{zi}}{\partial x_i} \right)^2 + \nu_z \left( \frac{\partial A_{yi}}{\partial x_i} - \frac{\partial A_{xi}}{\partial y_i} \right)^2 \right] \nu_i \end{aligned} \quad (26)$$

From this the inductance of the source, regardless of its shape and distribution, can be written as

$$L = 2W/I_s^2 \quad (27)$$

where  $I_s$  is the current in the source (coil).

The calculation of the resistive part of the system is based on the eddy current distribution. The dissipated energy in a finite element is<sup>[7]</sup>

$$P_i = \nu_i |J_{ei}|^2 / \sigma \quad (28)$$

Here  $J_{ei}$  is the resultant eddy current density in a finite element and can be written as

$$J_{ei} = -j\omega\sigma A_{ci} \quad (29)$$

where  $A_{ci}$  is the centroidal value of the magnetic vector potential and is calculated similarly to the 2D or axisymmetric case. The element used here is an eight-node brick and therefore the average is done over eight values for each component of  $A$  and the resultant absolute value of  $A$  is calculated. Thus substituting Equation (29) into Equation (28) and summing over all the elements in the finite element mesh yields the total dissipated energy

$$P = \sum_{i=1}^N P_i = \sum_{i=1}^N \nu_i \sigma \omega^2 |A_{ci}|^2 \quad (30)$$

The source resistance now becomes

$$R = P/I_s^2 \quad (31)$$

and the source impedance can be written as

$$Z = R + j\omega L = \frac{1}{I_s^2} (P + j\omega 2W) \quad (32)$$

In the 3D magnetostatic case only the stored energy term exists in the original equation and therefore only the source inductance can be calculated. (The source resistance is zero since it is assumed in the finite element formulation that the source is perfectly conducting.)

The considerations above are equally applicable to two-dimensional and axisymmetric problems. In 2D applications, assuming that the source current density is in the  $z$  direction, only  $B_x$  and  $B_y$  exist in Equation (25):

$$B_x = \frac{\partial A}{\partial y} \quad (33)$$

$$B_y = -\frac{\partial A}{\partial x}$$

and Equation (26) can be written as

$$W = \frac{1}{2} \sum_1^N \left[ \nu_x \left( \frac{\partial A}{\partial y} \right)^2 + \nu_y \left( \frac{\partial A}{\partial x} \right)^2 \right] \Delta_i \quad (34)$$

without any change in Equation (30) other than the calculation of  $A_{ci}$  in an element with a different number of nodes (Equation (9), (11) or (13)). In this equation  $\Delta_i$  is the area of element  $i$  since the depth is assumed to be unity.

In axisymmetric geometries the source is assumed to be in the positive  $\phi$  direction with field components in the  $r$  and  $z$  directions. Thus Equation (25) becomes<sup>[7]</sup>

$$\begin{aligned} B_r &= -\frac{\partial A}{\partial z} \\ B_z &= \frac{A}{r} + \frac{\partial A}{\partial r} \end{aligned} \quad (35)$$

and, by introducing the volume as  $\nu_i = 2\pi r_{ci} \Delta_i$ , Equation (26) becomes

$$W = \pi \sum_1^N \left[ \nu_r \left( \frac{\partial A}{\partial z} \right)^2 + \nu_z \left( \frac{A}{r} + \frac{\partial A}{\partial r} \right)^2 \right] \Delta_i r_{ci} \quad (36)$$

where  $r_{ci}$  is the centroidal distance from the symmetry line and is calculated using Equation (10) or (12).

Equation (30) remains unchanged other than the introduction of  $\nu_i$  above.

Thus the inductance of a coil or any other configuration of sources can be calculated from the distribution of the magnetic vector potential, regardless of the geometry and source distribution. There are, however, three problems associated with this approach.

- The calculation of the reactive term requires space differentiation of the magnetic vector potential. This is by itself a simple task since it can be done in the finite element program with little extra computational effort<sup>[5]</sup>. The problem is one of accuracy, since differentiation of an approximate solution may introduce errors, especially if the discretization of the geometry is relatively coarse. This, as will be shown later, is especially important in 3D calculations. The calculation of the resistive part poses no such difficulty since it is calculated directly from the magnetic vector potential.

The flux density  $B$  is not known and has to be calculated from  $A$ :

$$\begin{aligned} B_x &= \frac{\partial A_z}{\partial y} - \frac{\partial A_y}{\partial z} \\ B_y &= \frac{\partial A_x}{\partial z} - \frac{\partial A_z}{\partial x} \\ B_z &= \frac{\partial A_y}{\partial x} - \frac{\partial A_x}{\partial y} \end{aligned} \quad (25)$$

Substituting this in Equation (24) and summing over all the elements in the solution region yields the total stored energy in the system:

$$\begin{aligned} W &= \frac{1}{2} \sum_1^N \left[ \nu_x \left( \frac{\partial A_{zi}}{\partial y_i} - \frac{\partial A_{yi}}{\partial z_i} \right)^2 \right. \\ &\quad \left. + \nu_y \left( \frac{\partial A_{xi}}{\partial z_i} - \frac{\partial A_{zi}}{\partial x_i} \right)^2 + \nu_z \left( \frac{\partial A_{yi}}{\partial x_i} - \frac{\partial A_{xi}}{\partial y_i} \right)^2 \right] \nu_i \end{aligned} \quad (26)$$

From this the inductance of the source, regardless of its shape and distribution, can be written as

$$L = 2W/I_s^2 \quad (27)$$

where  $I_s$  is the current in the source (coil).

The calculation of the resistive part of the system is based on the eddy current distribution. The dissipated energy in a finite element is<sup>[7]</sup>

$$P_i = \nu_i |J_{ei}|^2 / \sigma \quad (28)$$

Here  $J_{ei}$  is the resultant eddy current density in a finite element and can be written as

$$J_{ei} = -j\omega\sigma A_{ci} \quad (29)$$

where  $A_{ci}$  is the centroidal value of the magnetic vector potential and is calculated similarly to the 2D or axisymmetric case. The element used here is an eight-node brick and therefore the average is done over eight values for each component of  $A$  and the resultant absolute value of  $A$  is calculated. Thus substituting Equation (29) into Equation (28) and summing over all the elements in the finite element mesh yields the total dissipated energy

$$P = \sum_{i=1}^N P_i = \sum_{i=1}^N \nu_i \sigma \omega^2 |A_{ci}|^2 \quad (30)$$

The source resistance now becomes

$$R = P/I_s^2 \quad (31)$$

and the source impedance can be written as

$$Z = R + j\omega L = \frac{1}{I_s^2} (P + j\omega 2W) \quad (32)$$

In the 3D magnetostatic case only the stored energy term exists in the original equation and therefore only the source inductance can be calculated. (The source resistance is zero since it is assumed in the finite element formulation that the source is perfectly conducting.)

The considerations above are equally applicable to two-dimensional and axisymmetric problems. In 2D applications, assuming that the source current density is in the  $z$  direction, only  $B_x$  and  $B_y$  exist in Equation (25):

$$B_x = \frac{\partial A}{\partial y} \quad (33)$$

$$B_y = -\frac{\partial A}{\partial x}$$

and Equation (26) can be written as

$$W = \frac{1}{2} \sum_1^N \left[ \nu_x \left( \frac{\partial A}{\partial y} \right)^2 + \nu_y \left( \frac{\partial A}{\partial x} \right)^2 \right] \Delta_i \quad (34)$$

without any change in Equation (30) other than the calculation of  $A_{ci}$  in an element with a different number of nodes (Equation (9), (11) or (13)). In this equation  $\Delta_i$  is the area of element  $i$  since the depth is assumed to be unity.

In axisymmetric geometries the source is assumed to be in the positive  $\phi$  direction with field components in the  $r$  and  $z$  directions. Thus Equation (25) becomes<sup>[7]</sup>

$$\begin{aligned} B_r &= -\frac{\partial A}{\partial z} \\ B_z &= \frac{A}{r} + \frac{\partial A}{\partial r} \end{aligned} \quad (35)$$

and, by introducing the volume as  $\nu_i = 2\pi r_{ci} \Delta_i$ , Equation (26) becomes

$$W = \pi \sum_1^N \left[ \nu_r \left( \frac{\partial A}{\partial z} \right)^2 + \nu_z \left( \frac{A}{r} + \frac{\partial A}{\partial r} \right)^2 \right] \Delta_i r_{ci} \quad (36)$$

where  $r_{ci}$  is the centroidal distance from the symmetry line and is calculated using Equation (10) or (12).

Equation (30) remains unchanged other than the introduction of  $\nu_i$  above.

Thus the inductance of a coil or any other configuration of sources can be calculated from the distribution of the magnetic vector potential, regardless of the geometry and source distribution. There are, however, three problems associated with this approach.

- The calculation of the reactive term requires space differentiation of the magnetic vector potential. This is by itself a simple task since it can be done in the finite element program with little extra computational effort<sup>[5]</sup>. The problem is one of accuracy, since differentiation of an approximate solution may introduce errors, especially if the discretization of the geometry is relatively coarse. This, as will be shown later, is especially important in 3D calculations. The calculation of the resistive part poses no such difficulty since it is calculated directly from the magnetic vector potential.

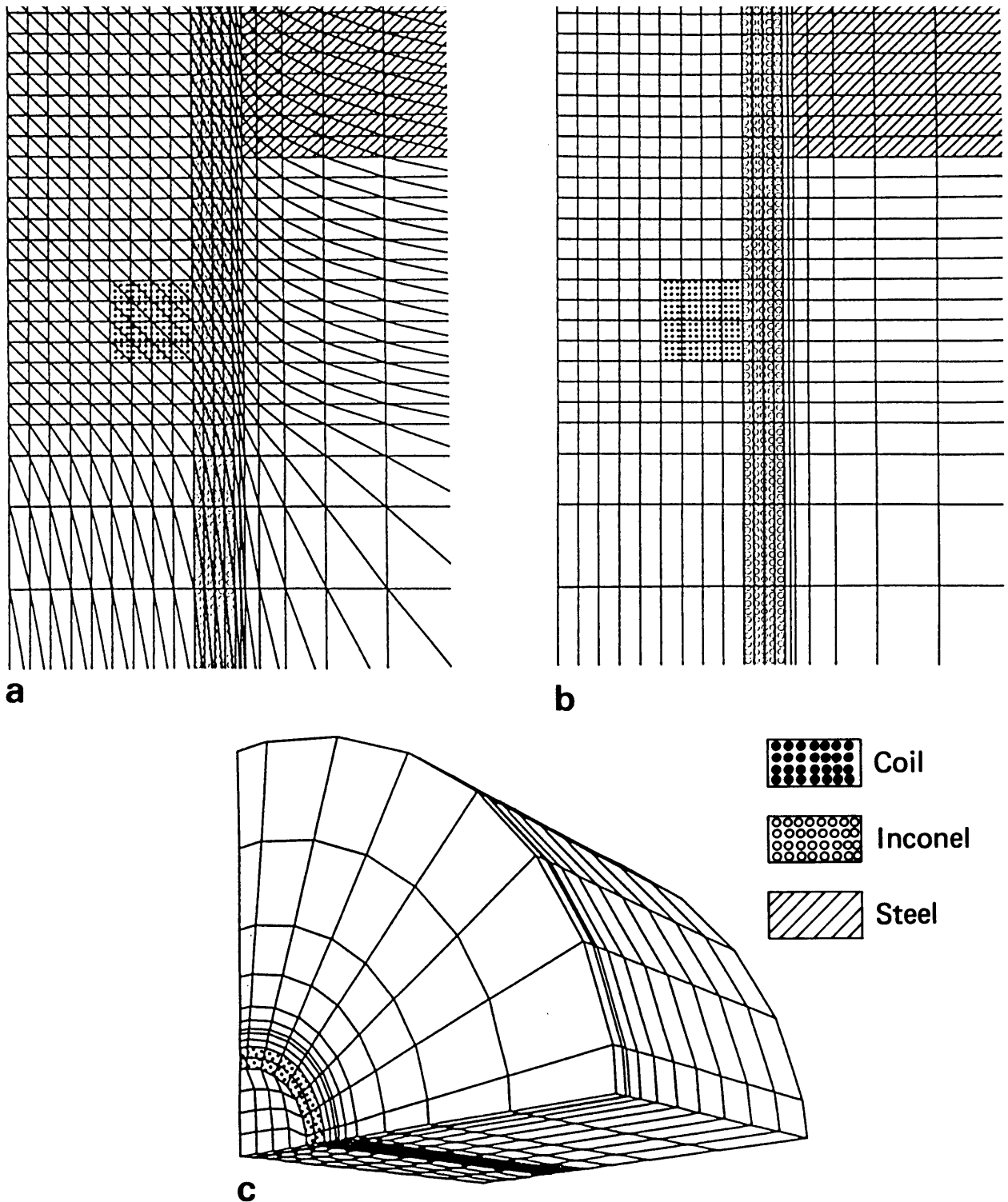


Fig. 3 Axisymmetric and 3D meshes used. The Inconel and tube regions are the same as in Figure 4. (a) Triangular element mesh (6000 elements, 3146 nodes); (b) Quadrilateral element mesh (3000 elements, 3146 nodes); (c) 3D hexahedral element mesh (1040 elements, 1346 nodes, 4092 variables)

### Comparison of triangular and quadrilateral elements

In order to explore further the effect of the choice of elements for the solution, the geometries shown in Table 2 were modelled using the finite element meshes in Figure 3. The self-inductance of the coil is calculated, but, unlike the results in Table 1, no analytical results exist except for the first geometry which has already been discussed in the previous paragraph. Considering first the results for the direct calculation of self-inductance in columns 2 and 4,

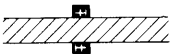
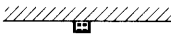

the results for the quadrilateral element are consistently higher by as much as 10% depending on the geometry. (The error percentage shown in column 4 compares this column to column 2).

The differences between calculating the inductance from energy considerations or direct integration are small, as indicated by the differences in columns 2 and 4. Again in the triangular element case the errors are lower because of the fact that the number of points at which the flux is calculated is double that for the quadrilateral elements.

**Table 1. Comparison of inductance of a coil in air with the theoretical value. All errors are with respect to the analytical solution, and inductances are in mH**

Analytic	Triangular Energy		Quadrilateral Energy		3D Energy	
	Direct	Energy	Direct	Energy	Energy	
0.78764579	0.757327 3.85%	0.758028 3.76%	0.761405 3.33%	0.757120 3.87%	0.705309 10.45%	Eddy current
	0.756447 3.96%	0.755220 4.11%	0.761084 3.37%	0.755020 4.14%	0.716817 8.99%	Magnetostatic

**Table 2. Comparison of inductances of various geometries. All errors are with respect to the second column and inductances are in mH**

Geometry	Triangular Energy		Quadrilateral Energy		3D Energy
	Direct	Energy	Direct	Energy	Energy
Coil in air	0.757327	0.758028 0.09%	0.761405 0.54%	0.757120 0.56%	0.705309 6.87%
	0.349953	0.349641 0.09%	0.353479 1.00%	0.350610 0.80%	
	0.544888	0.544966 0.01%	0.547199 0.42%	0.543830 0.61%	
	0.426203	0.426358 0.04%	0.429755 0.83%	0.426467 0.76%	0.473780 11.16%

Thus again, although the solution in terms of the magnetic vector potential is more accurate for the quadrilateral elements, the error introduced by calculating the self-inductance from energy considerations is lower in the triangular element case.

The 3D result in the last row is again within the same error limits as for the coil in air, indicating a mesh that is too coarse.

#### Calculation of differential impedances from energy considerations

As discussed earlier, using energy considerations to calculate inductances and impedances results in values that do not reflect the actual source distribution. Thus, in general, a differential eddy current probe cannot be modelled using this method.

In the particular case where the two coils are identical and linearity can be assumed, it is possible to derive the differential impedance from that of a single-coil (absolute) probe. The two coils in Figure 4 can be viewed as two different positions of a single coil, since the conditions around coil 2 are identical if coil 1 is moved to this location. Thus, if the impedance of a coil is calculated to correspond to the position of coil 1 and then, separately, to coil 2, the differential impedance of the arrangement in Figure 4 is the difference between the two impedances calculated above. Performing such calculations only requires the assumption of superposition, which is implicit in a linear system.

In modelling NDT phenomena where an absolute or differential eddy current probe is moved past a discontinuity, a relatively large number of probe positions needs to be modelled. It is however sufficient to calculate the impedance of an absolute probe and then, if necessary, the differential impedance can be derived from the

impedance of the absolute probe.

To confirm this, the geometry in Figure 4 was modelled using the meshes in Figure 3. It consists of an Inconel 600 tube (22.2 mm in diameter, 1.27 mm wall thickness) inside a 19.1 mm thick carbon steel plate with a gap of 0.38 mm between the tube and the steel.

The impedance plane trajectory of this geometry is shown in Figure 5a. It is a plot of 70 probe positions in the complex plane and describes the probe movement from some distance away to the middle of the steel plate. (Because of symmetry about the centre of the plate, a symmetric loop is described by moving the probe past the steel plate to some distance away from the plate.) The

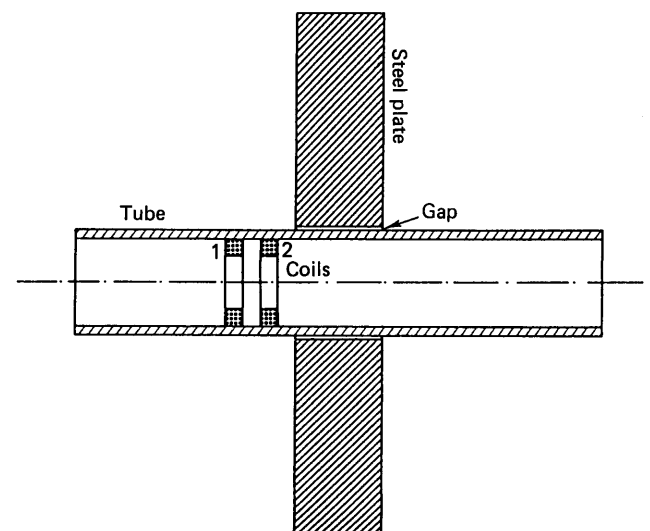


**Fig. 4** Geometry of steam generator testing problem including a differential eddy current probe

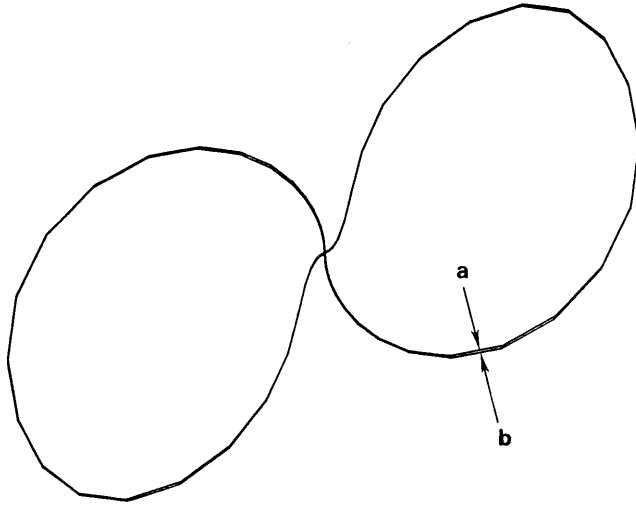


Fig. 5 Impedance plane trajectories obtained from axisymmetric calculations: (a) by modelling the differential eddy current probe; (b) by subtracting appropriate absolute probe position impedances

same result can be obtained by calculating the impedance of a single coil moving from the first position of coil 1 to the last position of coil 2 in Figure 4. Thus by calculating 78 absolute probe positions and subtracting the appropriate impedances, the differential impedance is obtained as

$$Z_d(i) = Z_{a(i+s)} - Z_{a(i)} \quad (39)$$

The impedance calculated in this way is plotted in Figure 5b. The two trajectories are almost indistinguishable, although differences of up to 0.8% exist in individual probe position impedances.

This method allows the calculation of differential impedances in 3D applications using energy considerations.

## Conclusions

Calculation of impedances or inductances of coils in axisymmetric geometries can be done by direct integration over the coils' cross sections or by calculating the dissipated and stored energy in the solution region. Both methods produce good results but, when energy considerations are utilized, the calculated inductance or impedance reflects the source as a whole and it is, in general, impossible to calculate the impedance of a single coil in a system of coils. In addition, the phase information is lost and the need to calculate spatial derivatives of the magnetic vector potential may introduce additional errors, especially for coarse discretization.

Because of these difficulties, there is little or no incentive to calculate inductances or impedances in axisymmetric geometries from energy considerations.

The use of different elements like the four-node quadrilateral element can produce improved results in terms of the magnetic vector potential but not necessarily in the final result. When calculating impedances from the magnetic vector potential, the number of elements in the source cross section is of prime importance. Thus using a large number of less sophisticated elements can produce superior results for the same discretization levels.

In three-dimensional geometries the energy approach is

the only possible method of calculating inductances and impedances. In linear problems it is also possible to calculate the differential impedance of eddy current probes from the impedance of a single coil. This is a crucial point for the successful application of 3D numerical models to NDT problems.

## Appendix. A note on uniqueness of solution

The solutions of the 2D and axisymmetric equations in (4)–(7) use the one-component magnetic vector potential formulations<sup>[1,4]</sup>. In all of these the Coulomb gauge is used to arrive at the form given<sup>[1]</sup>.

For 3D applications the divergence of the magnetic vector potential is not necessarily zero and there is some doubt whether the solution obtained through the magnetic vector potential is unique.

There are two main methods of overcoming this difficulty, short of explicitly imposing a gauge:

- the use of a modified vector potential<sup>[10–12]</sup>
- the use of isoparametric finite elements and properly specified boundary conditions<sup>[13]</sup>

The second of these methods was used to produce the results in this work and the first was used to verify the uniqueness of the solution.

Isoparametric finite elements use product shape functions which in turn guarantee that the magnetic vector potential is uniquely interpolated to the boundaries of the mesh<sup>[13]</sup>. This method will guarantee a unique solution provided that the boundary conditions are specified correctly.

A different approach is to view the 3D field equations (Equation (1) or (2)) as follows:

$$\nu \nabla \times \nabla \times \mathbf{A} = -\partial \mathbf{A} / \partial t - \nabla \phi \quad (40)$$

By defining a modified vector potential

$$\mathbf{A}^* = \mathbf{A} + \int \nabla \phi dt \quad (41)$$

this equation becomes

$$\nu \nabla \times \nabla \times \mathbf{A}^* = -\sigma \partial \mathbf{A}^* / \partial t \quad (42)$$

or, for the steady-state excitation,

$$\nu \nabla \times \nabla \times \mathbf{A}^* = -j\omega \sigma \mathbf{A}^* \quad (43)$$

where an implicit gauge  $\nabla \cdot \sigma \mathbf{A}^* = 0$  is satisfied.

This particular form of the equation is only valid in conducting regions of the solution domain. In non-conducting regions a magnetic scalar potential is used:

$$\mathbf{H} = -\nabla \psi \quad (44)$$

and, from the divergence of  $\mathbf{B}$ , the equation to be solved is

$$\nabla \cdot \mu \nabla \psi = 0 \quad (45)$$

The solution for the magnetic vector and scalar potentials must be matched on the interface between conducting and non-conducting regions. Both the formulation and boundary matching are described in detail elsewhere<sup>[10,11]</sup>.



For the purpose of this work it is important to note that all calculations in Equation (8)–(36) remain essentially the same. The magnetic vector potential is replaced with  $A^*$  in conductors. The field in non-conducting regions is calculated directly from the gradient of the magnetic scalar potential in Equation (44).

As mentioned above, this method was used to verify the results presented which were calculated using the magnetic vector potential alone. Although one could argue that the modified vector potential is a better choice for general field problems, in 3D NDT applications it is often necessary to describe complex, arbitrarily shaped defects, thus complicating the interface conditions. The vector potential is therefore used throughout the solution region and the uniqueness is guaranteed through the choice of element shape functions and boundary conditions.

## References

- 1 **Hammond, P.** 'Use of potentials in calculation of electromagnetic fields' *IEE Proc* **129** Part A 2 (1982) pp 106–112
- 2 **Silvester, P. and Chari, M.V.K.** 'Finite element solution of saturable magnetic field problems' *IEEE Trans Power Appar & Syst* **PAS-89** 7 (1970) pp 1642–1651
- 3 **Chari, M.V.K.** 'Finite element solution of eddy current problems in magnetic structures' *IEEE Trans Power Appar & Syst* **PAS-93** (1973) pp 62–72
- 4 **Palanisamy, R. and Lord, W.** 'Finite element modeling of electromagnetic NDT phenomena' *IEEE Trans Magn* **MAG-15** 6 (1979) pp 1479–1481
- 5 **Demerdash, N.A., Mohammed, O.A., Nehl, T.W., Fouad, F.A. and Miller, R.H.** 'Solution of eddy current problems using three dimensional finite element complex magnetic vector potential' *IEEE Trans Power Appar & Syst* **PAS-101** (1982) pp 4222–4229
- 6 **Ida, N. and Lord, W.** '3-D finite element predictions of magnetostatic leakage fields' *IEEE Trans Magn* **MAG-19** 5 (1983) pp 2260–2265
- 7 **Ida, N.** 'Three dimensional finite element modeling of electromagnetic nondestructive testing phenomena' *Ph D Dissertation* Colorado State University (Spring 1983)
- 8 **Palanisamy, R.** 'Finite element modeling of eddy current nondestructive testing phenomena' *Ph D Dissertation* Colorado State University (Summer 1980)
- 9 **Welsby, V.G.** *The theory and design of inductance coils* John Wiley and Sons, Inc, New York (1960) pp 42–44
- 10 **Morisue, T.** 'Magnetic vector potential and electric scalar potential in three-dimensional eddy current problem' *IEEE Trans Magn* **MAG-18** 2 (1982) pp 531–535
- 11 **Emson, C.R.I. and Simkin, J.** 'An optimal method for 3-D eddy currents' *IEEE Trans Magn* **MAG-19** 6 (1983) pp 2450–2452
- 12 **Polak, S.J., Wachters, A.J.H. and van Welij, J.S.** 'A new 3-D eddy current model' *IEEE Trans Magn* **MAG-19** 6 (1983) pp 2447–2449
- 13 **Biddlecombe, C.S., Heighway, E.A., Simkin, J. and Trowbridge, C.W.** 'Methods for eddy current computation in three dimensions' *IEEE Trans Magn* **MAG-18** 2 (1982) pp 492–497

## Author

The author is in the Electrical Engineering Department, The University of Akron, Akron, Ohio 44325, USA.

Paper received 29 June 1987. Revised 26 October 1987

